Currents and turbulence in and near mid-latitude sporadic E-layers caused by strong acoustic impulses

V. A. Liperovsky, C.-V. Meister, K. Schlegel, C. Haldoupis

HAL Id: hal-00316279
https://hal.science/hal-00316279

Annales
Geophysicae

Currents and turbulence in and near mid-latitude sporadic E-layers caused by strong acoustic impulses

V. A. Liperovsky[1], C.-V. Meister[2], K. Schlegel[3], C. Haldoupis[4]

[1] United Institute of Physics of the Earth Moscow, Russia
[2] Plasma Physics Project of the Institute for Theoretical Physics and Astrophysics at Potsdam University, Germany
[3] Max-Planck-Institute for Aeronomie, Katlenburg-Lindau, Germany
[4] University of Crete, Iracleon, Greece

Abstract. The generation of Hall and field-aligned currents in and in the vicinity of nighttime mid-latitude sporadic E-layers moving under the action of strong acoustic impulses of seismic, anthropogenic, or meteorological nature is considered in a model presented in this paper. The influence of the electrical polarization fields caused by charges at the horizontal edges of the sporadic layers and the finite conductivity of the external circuits are also taken into account. The theoretical model is applicable for ionospheric altitudes between 95 and 130 km. The estimates show that under certain conditions in a system with two sporadic E-layers, one of which is the current generator and the other is situated in the external circuit, the Farley-Buneman instability could be generated. On the other hand, observations show that Farley-Buneman waves are likely responsible for the infrequent echoes of mid-latitude 50-MHz backscatter with Doppler velocities near 300 m s^{-1}. The possibility exists that the proposed current-generator model is at the origin of the observed mid-latitude Farley-Buneman waves.

1 Introduction

One of the interesting phenomena of natural plasma clouds are the sporadic layers of enhanced ionization in the E-region of the ionosphere, called E_s-layers. The morphology of E_s-layers and the mechanisms of their creation under the action of horizontal wind shear have been studied for decades (Gershman *et al.*, 1976; Tshavdarov *et al.*, 1975; Whitehead, 1989). At mid-latitudes, E_s were mainly studied by ionosondes (Sprenger, 1981), rocket experiments (Andreeva *et al.*, 1971) and incoherent-scatter radars (Rowe, 1973) [see also Whitehead

(1989) for a review]. The existing evidence shows that at mid-latitude heights between 90 and 140 km intensive sporadic layers appear regularly, with their probability of occurrence depending on season. Further, the experimental investigation of the behavior of E_s characteristics before strong earthquakes and as a consequence of some military actions as well as strong anthropogenic activity in the vicinity of large industrial centers leads to the conclusion that remarkable E_s-layer anomalies may also exist (Liperovsky *et al.*, 1992), which demand an explanation.

Ionospheric sporadic E-layers are also associated with field-aligned irregularities. Long known by radio amateurs as a popular way of making long-distance VHF connections (Pocock, 1994), coherent backscatter from E_s-layers has been studied by several authors [see Haldoupis (1989) for a recent overview]. An example of a modern tool to investigate mid-latitude coherent backscatter is the SESCAT experiment in Crete, Greece (Haldoupis and Schlegel, 1993). This radar enables the registration of the backscatter Doppler spectrum, with its mean Doppler shift being an estimate of the irregularity phase velocity. The observed velocities at mid-latitudes are generally in the range of ± 100 m s^{-1}, but occasionally larger Doppler shifts around 300 m s^{-1} are also detectable. The irregularities corresponding to these large velocities are probably caused by the Farley-Buneman (FB) plasma instability, as argued in a recent paper by Schlegel and Haldoupis (1994). It is, however, not understood how such large electron drifts, corresponding to electric fields as large as 15 mV/m which are necessary in order to excite this instability, can be generated at mid-latitudes where the observed fields are much smaller.

During seismic and strong anthropogenic activity in the atmosphere acoustic waves have been observed using different radiophysical methods (Blanc, 1985; Toroshelidze and Fishkova 1988). Acoustic waves can also be generated in auroral electrojets and under special meteorological conditions such as severe weather, or can be excited by high-flying aircrafts.

In this paper a theoretical analysis is provided of the electromagnetic processes in dense (density n_s) E_s-layers of the nighttime mid-latitude ionosphere and its environment under the influence of strong acoustic waves with quasi-periods between 10 and 300 s. As the amplitudes of acoustic waves, propagating from the earth into the upper atmosphere of progressively lower density, constantly grow and the wave processes become almost nonlinear, an effective wave energy transfer to the E_s-layers and their environment takes place. The sporadic layers are considered here as plasma clouds moving in the ambient plasma of lower density $n_o < n_s$ in the presence of neutral winds which interact with the magnetized electrons and nonmagnetized ions, thus setting up electric fields and generating electric currents. It is assumed that under certain conditions, E_s-layers can cause spikes of electric field impulses and thus generate Hall, Pedersen, and field-aligned currents inside and near the layers. Further, if the velocity of the neutral wind is sufficiently strong, electrostatic turbulence waves of FB type can also be excited.

2 Current generator model of an E_s-layer

Following next is the scenario of the plasma processes in an E_s region. The nighttime mid-latitude E_s-layers are known to contain large concentrations of metallic ions ($Fe^+, Mg^+, Al^+, K^+, Ca^+$) in addition to the usual O_2^+ and NO^+ ions. Other typical E_s parameters are: charged particle density $n_s \approx 10^4$ cm^{-3}, vertical width 100–500 m, and horizontal extent of about 50–100 km (Fatkullin *et al.*, 1981). By taking the inclination α of the geomagnetic field into account and remarking that the wave vector of the acoustic waves is elevated with an angle β, which is high enough to guarantee weak wave damping and minimal reflection, we can assume that the velocity components of the neutral particles parallel and perpendicular to the geomagnetic field are comparable.

As the possible sources of electrical current generation are the neutral winds, obviously maximum ion velocities V^A seem to be reached at altitudes with yet $v_{in} \leq \omega_{Bi}$, i.e., at altitudes $h \sim 120$ km. At larger altitudes fewer ions are carried away by neutral winds. Taking into account that the magnitude of acoustic waves propagating up from the earth's surface through the neutral atmosphere grows and that in the E region at the altitude $h \cong 100$ km the amplitude of the velocity oscillations of acoustic waves may reach values of 80 m s^{-1}, one can assume that acoustic pulses at $h = 120$ km have a magnitude which is approximately (without nonlinear and damping effects) $\sim 1/\sqrt{n}$ times larger than the magnitude at $h = 100$ km and reaches values of the order of 150–200 m s^{-1}; n is the density of the neutral atmosphere. This hypothesis corresponds to the results of Tsunoda *et al.* (1993). Therefore we propose a possible model of current generation, when two sporadic E-layers occur simultaneously at different altitudes. One E_s-layer is a current generator, the other is a load. In the "E_s load" a maximum current will be generated if the "E_s generator" is placed at an altitude of

$h = 120$–130 km. Certainly, the existence of two sporadic layers at the discussed altitudes is a rare phenomenon.

Next, consider a situation with a half wavelength of the acoustic wave which is somewhat larger than the dimension of the E_s-layer generator in the wave propagation direction, so that the layer interacts with the positive wave phase. In this case the wave period is larger than 10 s (besides, waves with very low periods are strongly damped) and lower than the Brünt-Väissälä period $T_B \approx 500$ s. Further, it is assumed that the interaction of the acoustic wave with the lower lying "E_s load" is negligible. Figure 1 illustrates the scheme of the proposed model.

In order to relate the E_s generator–E_s load model to SESCAT some more remarks have to be made. For an arbitrary direction of the acoustic wave, the wave vector $\vec{k}^A$ can be represented as the sum of two components, one perpendicular to the earth's geomagnetic induction $\vec{B}_o$ and one parallel, $\vec{k}^A = \vec{k}_\perp^A + \vec{k}_\parallel^A$. The component of the acoustic wave parallel to $\vec{B}_o$ in the sporadic layer generator does not have any significant effect on the plasma, even when the wave velocity parallel to $\vec{B}_o$ is of the order of the sound velocity. That is why we study only the momentum transfer of the perpendicular to $\vec{B}_o$ wave component $\vec{k}_\perp^A$ to the sporadic layer. Consider the special case when $\vec{k}_\perp^A$ (and also $\vec{V}_{n\perp}^o$) is situated in the same plane as the vectors $\vec{B}_o \parallel \vec{n}_z$ and the vertical. Choosing the $\vec{n}_x$-axis parallel to $\vec{k}_\perp^A$, the vector $\vec{n}_y$ will be located in the horizontal plane parallel to the sporadic layer and points to the reader (Fig. 2). Thus $\vec{k}_\perp^A$ points along the $\vec{n}_x$ direction and the anticipated small-scale electrostatic FB waves propagate in the $\vec{n}_x$ direction, which is parallel to the line-of-sight of SESCAT. Thus the electrostatic waves are detectable. As a second case
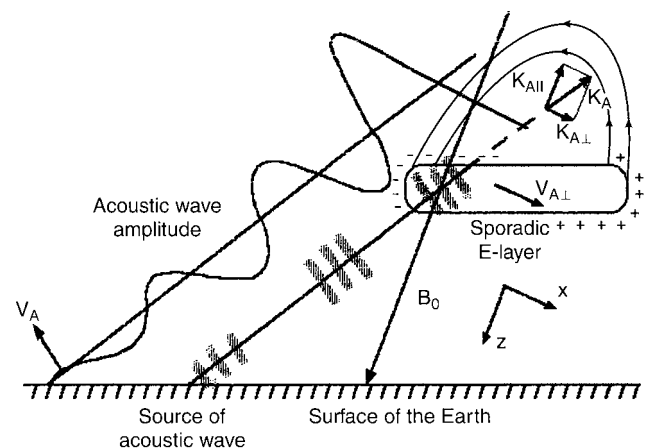

Fig. 1. Acoustic wave reaching the E region and causing an neutral-wind spike. $\vec{V}_\perp^A$ designates the component of neutral wind-velocity perpendicular to the geomagnetic field $\vec{B}_o$. The neutral wind generates electrical currents in the E_s-layer, which are closed by currents in the environmental plasma of the E region or by currents in a further E_s-layer connected with the first E_s-layer by the same geomagnetic field lines. The system of field-aligned and perpendicular to $\vec{B}_o$ currents is three-dimensional. Currents perpendicular to the plane of the figure are not shown
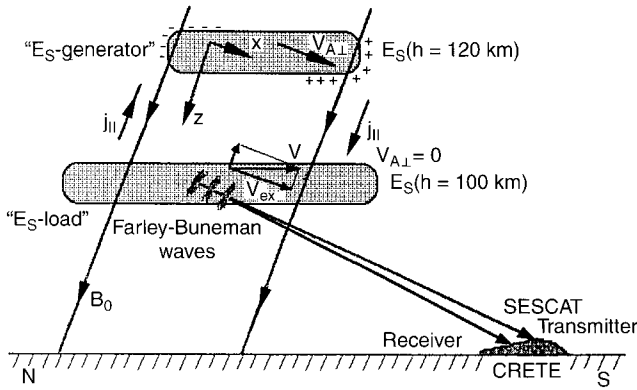
Fig. 2. Scheme to interpret the SESCAT experiment on the basis of the model E_s generator–E_s load: two sporadic layers are situated at different altitudes, for example, one layer is placed at the altitude $h = 120$ km and the other lies at $h = 100$ km. Optimal conditions for the generation of Farley-Buneman turbulence exist when the acoustic wave acts on the upper E_s-layer (E_s generator) and the amplitude of the acoustic wave is large ($V^A \approx C_s$. In the lower layer (E_s load) the amplitude of the acoustic wave is small, $V^A \approx 0$)

we suggest that $\vec{k}_\perp^A$ is perpendicular to the $\vec{B}_o$ vertical plane. Consequently, $\vec{k}_\perp^A$ lies in a horizontal plane parallel to the west-east direction. Assuming that $\vec{k}_\perp^A$ is directed along the $\vec{n}_y$-axis and points eastward, the possible FB waves propagate in the $\vec{n}_y$ direction, which is perpendicular to the line-of-sight of the SESCAT experiment in Crete, and the FB waves are not detectable. Thus the first case is optimal for the SESCAT experiment interpretation.

Thus the main features of the current and FB-wave generation will be studied with the help of the following simple model illustrated in Fig. 3, in which a homogeneous plasma cloud with the form of a parallelepiped is shown, extending perpendicular to the earth's magnetic field $\vec{B}_o \parallel \vec{n}_z$ directed along the z-axis (i.e., z-axis points
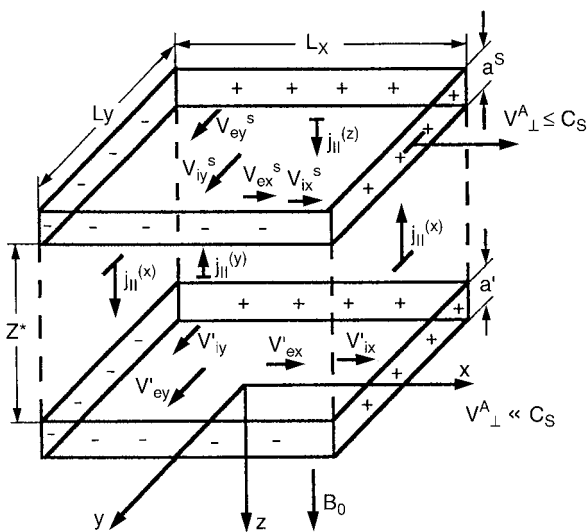
Fig. 3. Schematic picture of the model E_s generator–E_s load. The neutral wind acts on the upper layer (E_s generator) and does not act on the lower layer (E_s load). In the lower layer rather large electron velocity drifts V_{ex} with respect to the ions can occur

downwards). Under the action of the acoustic wave the ions move in the x direction, $\vec{V}^A \parallel \vec{n}_x$ and at the x-edge of the E_s-layer a positively charged particle cloud (and an E_x-field) appears. As a result of the Lorentz force a negatively charged cloud is formed at the y-edge and an E_y-field occurs. The electron current inside the E_s-layer is closed by Pedersen, Hall, and field-aligned currents in the plasma layers near the E_s-layer generator or in the second lower-lying sporadic E_s-layer, which is the "E_s-load". Thus in this model effects of the external circuit are taken into account. Similar treatments of an external circuit with model electric conductivity were partially done by Völk and Haerendel (1971) for ionospheric plasma clouds above the E region and by Jacobson and Bernhardt (1985), who also considered electrostatic effects on plasma layers during acoustic wave influence.

Taking the formation of charged layers and the polarization fields E_y and E_x into account, the system of equations of motion for the plasma particles in the generator and load layers reads as follows. For the upper floor (E_s generator, $h = 120$ km, $V^A \leq 300$ m s^{-1}) one has

$$0 = q_e E_x^s - m_e \omega_{Be} V_{ey}^s, \tag{1}$$

$$0 = q_e E_y^s + m_e \omega_{Be} V_{ex}^s, \tag{2}$$

$$0 = q_i E_x^s - m_i v_{in}^s (V_{ix}^s - V^A) + m_i \omega_{Bi}^s V_{iy}^s, \tag{3}$$

$$0 = q_i E_y^s - m_i v_{in}^s V_{iy}^s - m_i \omega_{Bi}^s V_{ix}^s. \tag{4}$$

Here we assume that a linear dependence between the electric fields in the lower ($\vec{E}'$) and upper ($\vec{E}^s$) layers exists,

$$E_x' = \kappa_x E_x^s, \tag{5}$$

$$E_y' = \kappa_y E_y^s. \tag{6}$$

The values of the coefficients $\kappa_x \leq 1$ and $\kappa_y \leq 1$ depend on the geometry and altitude of the load layer. Really the coefficients κ_x and κ_y have to be calculated solving the current continuity equation for the two-floor system taking into account the voltage drop along the field-aligned currents. In this work supposed values of κ_x and κ_y are used.

The motion in the lower layer – E_s load (in general it is the plasma of the nighttime E region) is given by

$$0 = q_e \kappa_x E_x^s - m_e \omega_{Be} V_{ey}', \tag{7}$$

$$0 = q_e \kappa_y E_y^s + m_e \omega_{Be} V_{ex}', \tag{8}$$

$$0 = q_i \kappa_x E_x^s - m_i v_{in}' V_{ix}', \tag{9}$$

$$0 = q_i \kappa_y E_y^s - m_i v_{in}' V_{iy}'. \tag{10}$$

The geometry of the sporadic E-layer as a current generator shown in Fig. 3 forms the framework for the theoretical calculations made in the paper. The thickness of the E_s generator is a^s and the thickness of the E_s load is described by a'; L_x and L_y are the horizontal dimensions of the clouds, and ΔL_x, ΔL_y are the

thicknesses of the field-aligned current sheets near the *x*- and *y*-edges of the E_s layers, respectively.

The total currents along both the *x*- and the *y*-axis in the two-layer system equal zero. It is suggested that there are no currents outside the layers. The equations for the currents read:

$$V_{iy}' + \xi V_{iy}^s = V_{ey}' + \xi V_{ey}^s, \tag{11}$$

$$V_{ix}' + \xi V_{ix}^s = V_{ex}' + \xi V_{ex}^s, \tag{12}$$

$$\xi = \frac{a^s n_s}{a' n'}. \tag{13}$$

Here m_α, n_α, q_α, $\vec{V}_\alpha$ denote the mass, density, charge, and mean velocity of particles of type α, $\alpha = e$ (electron), $\alpha = i$ (ion), $n_e = n_i$, $\vec{E}^s$ is the mean electrical field in the E_s-generator layer, $\vec{E}'$–in the E_s-load layer; $v_{\alpha n}$ represents the frequency of collisions between charges of type α and neutrals, $\omega_{B\alpha} = |q_\alpha| B_o/c m_\alpha$ is the Larmor frequency. The symbol "'" deals with the E_s load-layer, "s" – deals with the "E_s-generator" layer. At the considered atmospheric altitudes the ions are unmagnetized ($v_{in} \gg \omega_{Bi}$) in the E_s load. The particle temperatures are almost space independent. As a first approximation we neglect the space dependence of the densities too, also at the borders of the plasma clouds. Indeed, assuming $T_e \approx 250$ K and $L_n = 1/(\partial \ln n/\partial x) \approx 0.1$–1 km, the term proportional $V^A m_i v_{in}$ in Eq. 3 seems to be approximately two-three orders of magnitude larger than possible additional contributions proportional to the space gradient.

The necessary condition to neglect the currents in the transition layer between generator and load is $\xi_o^s = n'a'/n_o L_p \gg 1$, where L_p designates the vertical characteristic thickness of the ambient plasma region ($L_p \approx 50$ km).

Solving the system Eqs. 1–12 one finds for the dependence of the electron bulk velocity components in the sporadic layer on the neutral-wind velocity the relations

$$V_{ex}^s = \xi V^A \left\{ (\xi + \kappa_y) + \kappa_y \frac{\omega_{Bi}^{s\,2}}{v_{in}' v_{in}^s} + \frac{\kappa_x \kappa_y}{(\xi + \kappa_x)} \frac{\omega_{Bi}^{s\,2}}{v_{in}^{s\,2}} \right\}^{-1},$$

$$V_{ey}^s = - \xi \kappa_y V^A \left\{ (\xi + \kappa_y)(\xi + \kappa_x) \frac{v_{in}^s}{\omega_{Bi}^s} + \kappa_y(\xi + \kappa_x) \frac{\omega_{Bi}^s}{v_{in}'} \right.$$
$$\left. + \kappa_x \kappa_y \frac{\omega_{Bi}^s}{v_{in}^s} \right\}^{-1}. \tag{14}$$

Taking into account the conditions $v_{in}^s/\omega_{Bi}^s \gg 1$, $v_{in}'/v_{in}^s \gg 1$ and assuming $\kappa_x \leq 1$, $\kappa_y \leq 1$, $\xi \geq 1$ in zeroth-order approximation one can write

$$V_{ex}^s \approx \frac{V^A \xi}{\kappa_y + \xi}, \tag{15}$$

$$V_{ey}^s = - \frac{\kappa_y \omega_{Bi}^s}{(\xi + \kappa_x) v_{in}^s} V_{ex}^s,$$

$$V_{ix}^s = V^A - \frac{\xi^2 V^A}{(\xi + \kappa_x)(\xi + \kappa_y)} \frac{\omega_{Bi}^{s\,2}}{v_{in}^{s\,2}},$$

$$V_{iy}^s = \frac{-\kappa_y V^A}{\xi + \kappa_y} \frac{\omega_{Bi}^s}{v_{in}^s},$$

$$E_x^s = \frac{-\xi \kappa_y\, m_i\, V^A}{q(\xi + \kappa_x)(\xi + \kappa_y)} \frac{\omega_{Bi}^{s\,2}}{v_{in}^{s\,2}},$$

$$E_y^s = \frac{\xi\, m_i\, \omega_{Bi}^s\, V^A}{q(\xi + \kappa_y)}.$$

For the electron velocity in the E_s load one obtains

$$V_{ex}' \approx \frac{V^A \kappa_y \xi}{\kappa_y + \xi} \tag{16}$$

and $V_{ex}' \leq V^A \approx C_s$; C_s designates the sound velocity. This result gives a chance to explain the occurrence of FB turbulence during the experiments of Haldoupis and Schlegel. A more accurate analysis based on the current continuity equation seems not to give essential corrections.

It should be mentioned that at E-region altitudes the background electric field $\vec{E}_o$ is usually not large enough to produce FB turbulence, but in particular cases when the $\vec{E}_o$ field is westward directed and is added to the E_y' field of the E_s load, the total westward field can be strong enough to generate electron drift velocities with $V_{e\perp} \geq C_s$, so that the FB instability will be excited.

3 On the field-aligned currents

Now the problem of field-aligned currents in the system E_s generator–E_s load will be analyzed. First the *XZ*-section of the proposed two-floor current generator system is considered. Within the frame of the suggested model the regions near the corners of the sporadic layers, i.e., of both the E_s layer and the E_s generator are excluded from the analysis.

The current in the E_s generator along the *x*-axis proceeds in the field-aligned currents in the E_s load. The continuity condition of the whole current reads

$$J_x^s = |q|\, n_s\, a^s\, L_y\, (V_{ix}^s - V_{ex}^s) = j_\parallel L_y \Delta L_x. \tag{17}$$

Ohm's law for the field-aligned current is

$$j_\parallel = \sigma_\parallel \frac{U^x}{Z^*}, \tag{18}$$

where

$$U^x = L_x\, |E_x^s|(1 - \kappa_x)/2 \tag{19}$$

describes the potential difference along the geomagnetic field lines between E_s generator and E_s load; $\sigma_\parallel = q^2 n_o/m_e v_{en}$; Z^* is the characteristic distance between the layers along the magnetic field lines. Using Eqs. 17–19 and the formulas Eqs. 14,15 for V_{ex}^s, V_{ix}^s and E_x^s, one finds

$$\frac{1 - \kappa_x}{\xi + \kappa_x} = \frac{1}{\xi} \frac{2\, a_s\, Z^*}{\Delta L_x\, L_x} \frac{n_s}{n_o} \frac{v_{en}^s}{\omega_{Be}} \frac{v_{in}^s}{\omega_{Bi}^s}. \tag{20}$$

Further continuity equation and Ohm's law for the field-aligned currents in the YZ-section of the system E_s generator–E_s load are studied,

$$|q|\, n_s\, a^s\, L_x\, (V_{iy}^s - V_{ey}^s) = j_\parallel\, L_x\, \Delta L_y, \tag{21}$$

$$j_\parallel = \frac{q^2\, n_o}{m_e\, v_{en}}\, \frac{U^y}{Z^*}, \tag{22}$$

$$2\, U^y = L_y\, |E_y^s|\, (1 - \kappa_y). \tag{23}$$

From Eqs. 21–23 and the expressions for V_{ey}^s, V_{iy}^s and E_y^s one has

$$1 - \kappa_y = \frac{\kappa_x}{\xi + \kappa_x}\, \frac{\kappa_y}{\xi}\, \frac{2\, a_s\, Z^*}{\Delta L_y\, L_y}\, \frac{n_s}{n_o}\, \frac{v_{en}^s}{\omega_{Be}}\, \frac{\omega_{Bi}^s}{v_{in}^s}. \tag{24}$$

Finally, from Eqs. 20 and 24 κ_x and κ_y can be found. Assuming that the sporadic layers contain metallic ions, and thus $a^s = 2 \times 10^2$ m, $Z^* = 2 \times 10^4$ m, $\Delta L_x \approx \Delta L_y \sim 10^2$ m, $L_x \sim L_y \approx 10^5$ m, $n_s/n_o \approx 50$, $v_{en}^s/\omega_{Be} \simeq 10^{-3}$, $v_{in}^s/\omega_{Bi} \simeq 3$, and $\xi \approx 1$, it follows $\kappa_y \approx 0.99$ and $\kappa_x \approx 0.8$. Assuming $\xi \approx 10$ one has $\kappa_y \approx 0.99$ and $\kappa_x \approx 0.99$. More detailed parameter studies of the quasi-three-dimensional *E*-layer model for various geomagnetical conditions will be given in a further paper.

As mentioned, acoustic waves have been observed in the atmosphere using different radiophysical methods. Infrasound waves are found to be damped by kinematic viscosity at altitudes between 90 and 140 km (see review by Blanc, 1985), but according to atmospheric filtering effects waves with frequencies of 5×10^{-3} to 0.1 Hz may be able to propagate without severe attenuation. Indeed, series of infrasound oscillations with periods of $T = 10$–100 s were seen during seismic activity, and maximum amplitudes were found at about 150 km (Najita *et al.*, 1974). Also note that neutral-wind velocities V^A in the lower thermosphere at mid-latitudes in summer are of the order of 20–40 m s^{-1} (e.g., Manson *et al.*, 1990), but occasionally at altitudes of about 105 km, higher values of 80 m s^{-1} or more may occur.

Let us make some estimations. We assume $\xi > 1$ (then $\kappa_y \approx 1$) which is possible in cases when the E_s-generator layer is denser or thicker than the E_s-load layer. Suggesting $\xi = 10$ one has $V_{ex}' \approx 0.91 V^A$. For $\xi = 20$ one finds $V_{ex}' \approx 0.95 V^A$. Thus under optimum conditions with neutral-wind spikes of $V^A \approx 200$ m s^{-1}, the electron velocity amounts to $V_e' \approx 180$ m s^{-1}. If for optimum conditions, to the wind spikes a background wind of $V_o^A \approx 140$ m s^{-1} is added, one has an effective wind velocity of 340 m s^{-1} and $V_{ex}' \approx 0.91 \cdot 340$ m s^{-1} = 300 m s^{-1}. There can be also an additional effect of the external electric field, which value may be assumed to be 5 mV/m in the mid-latitude ionosphere. This external field can cause electron velocities of about 100 m s^{-1}. Thus, under very rare geophysical conditions with strong effective neutral-wind velocities the electron speeds can exceed the critical velocity for the generation of FB waves. Then these waves could contribute to the type-1 reflections observed in the SESCAT experiment.

A further possible secondary source of acoustic disturbances and neutral-wind spikes can be connected with the cells of scales of a few tens of kilometers occurring during the nonlinear evolution of gravity waves (Waltersheid *et al.*, 1988).

4 High doppler-velocity SESCAT events

A description of the SESCAT experiment has already been published (Haldoupis and Schlegel, 1993) and should not be repeated here. The backscatter spectra are on-line calculated and recorded with a time resolution of 4.8 s and frequency resolution of 1.2 s^{-1}, corresponding to a Doppler-velocity resolution of 3.6 m s^{-1}. In the subsequent data analysis these spectra can be further integrated in order to reduce the scatter. For each spectrum then the first four moments, i.e., backscattered power, Doppler shift, width, and skewness, are calculated. The Doppler velocities are usually in the range of ± 100 m s^{-1}, where the positive sign corresponds to a velocity towards the radar. Since the radar is looking almost northward at an elevation of 30°, a positive Doppler velocity means actually a velocity southward (with a downward component).

Figure 4 shows in the upper panel a SESCAT spectrum exhibiting an unusually large Doppler shift. It is plotted as a function of Doppler velocity rather than Doppler frequency in order to facilitate comparison with other coherent radars. The numbers in the upper right corner indicate the four moments of the spectrum: the backscattered power of 16.4 dB is of average magnitude, usually values between 3 and 25 are recorded. The Doppler velocity is -319.2 m s^{-1} and the width is 84.1 m s^{-1}. The dimensionless skewness parameter (1.5) indicates the asymmetry of the spectrum which is caused by the "tail" towards smaller Doppler velocities. For comparison a SESCAT spectrum of usual appearance has been plotted in the lower panel of Fig. 4. It is narrower, almost symmetric, and shows a Doppler velocity of -46.9 m s^{-1}. It should be noted that the majority of the recorded SESCAT spectra show a Doppler velocity of $|v_D| \leq 100$ m s^{-1} and a width between 50 and 150 m s^{-1}.

The spectrum in the upper panel of Fig. 4 resembles very much the type-1 spectra observed in the auroral zone or at the equator (e.g., Haldoupis, 1989), which are generally assumed to be caused by the FB instability. Although the actual threshold velocity to excite this instability is normally around 350–370 m s^{-1}, neutral winds as well as the presence of ions with masses greater 30–32 AMU (from meteors) can reduce this threshold. This has been discussed in detail by Schlegel and Haldoupis (1994), who came to the conclusion that SESCAT spectra with peak Doppler velocities around 300 m s^{-1} may be caused by the FB instability.

In the mean time 14 such high-velocity spectra have been recovered with SESCAT within the observational period of 2 years. No correlation with k_p was found, thus the high electric field necessary to produce the threshold drift velocity is most probably not of magnetospheric origin. A process as described in Sect. 2 may therefore be responsible for the excitation of the FB instability,
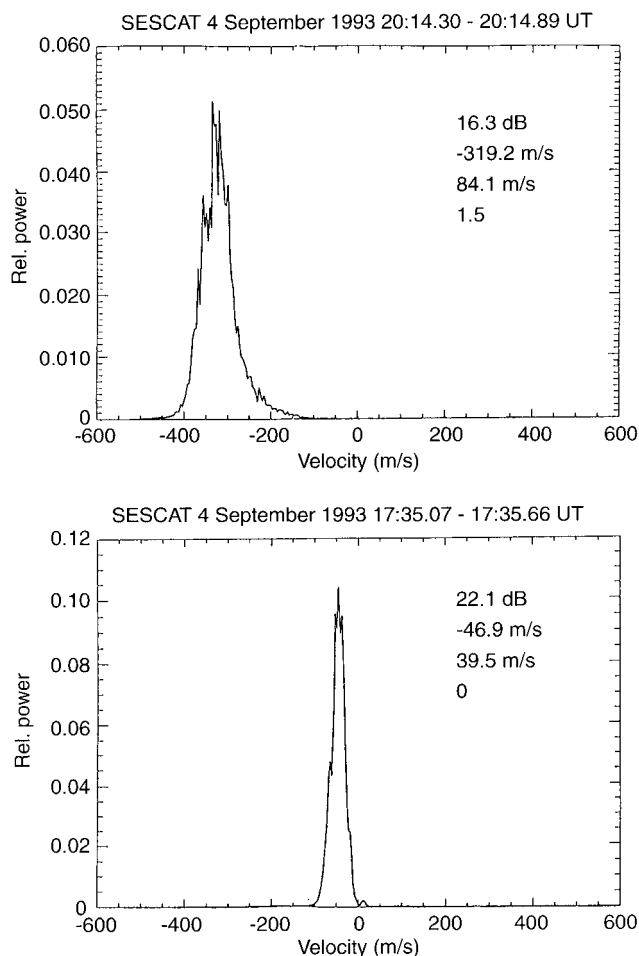
SESCAT 4 September 1993 20:14.30 - 20:14.89 UT

16.3 dB

-319.2 m/s

84.1 m/s

1.5

SESCAT 4 September 1993 17:35.07 - 17:35.66 UT

22.1 dB

-46.9 m/s

39.5 m/s

0

Fig. 4. Examples of SESCAT Doppler power spectra. The *lower panel* shows a commonly observed spectrum at small Doppler shifts. The largely shifted spectrum in the *upper panel* is identified with pure type-1 irregularities generated by the Farley-Buneman instability. Note that the latter spectral type is quite rare

which in turn causes the irregularities with unusually high Doppler velocity.

5 Discussion and concluding remarks

The generation of electron Hall and field-aligned currents in and in the vicinity of ionospheric E_s-layers by strong acoustic impulses, propagating from the surface of the earth into the ionosphere, was considered. The acoustic waves can be of a seismic, anthropogenic, or meteorological nature. The estimates within a quasi-three-dimensional model E_s generator–E_s load show that under certain conditions in the E_s-load-layer and in its surrounding plasma, a sufficiently large velocity $V^A_{\perp x}$ of an acoustic wave is capable of sustaining large electron drift velocities in the E_s-load-layer. This mechanism might be sufficient to excite the FB instability resulting in quasi-stationary turbulence.

Experimental evidence exists that shows large velocity electrostatic waves to be generated in the mid-latitude nighttime E region of the ionosphere. Indeed, in

the mid-latitude backscatter data obtained with SES-CAT, more than a dozen pure FB waves with phase velocities near 300 m s^{-1} were found within the summer period of 1993. In this regard, the excitation of mid-latitude FB waves can be regarded as a rather rare phenomenon, caused possibly by the current-generator mechanism presented in this paper.

In addition, according to estimates by Liperovsky and Meister (1995), the closure field-aligned currents in the external circuit can cause collisional heating of the electrons, and probably turbulent heating as well, especially in the torches above the edges of the sporadic layer. The physics of torches will be discussed in a separate paper. Also experiments on vertical sounding of E_s-layers, as discussed by Liperovskaya et al. (1994) and Alimov et al. (1989), show that at times the E_s-layer density decreases abruptly during strong seismic activity. This could be understood in the framework of the proposed current generation mechanism, if heating effects are also taken into account.

One more possible secondary source of acoustic disturbances and neutral-wind spikes may be connected with the cells of characteristic lengths of a few tens of kilometers, which appear during the process of nonlinear evolution of gravity waves (Walterscheid et al., 1988). But there are not enough experimental data for a more detailed comparison of the suggested current generator mechanism. At present, the proposed mechanism is not more than a possible one. Usually, the ambient (external) electric field in the E-layer ionosphere cannot result in electron drift velocities of the order of the sound velocity. But if an acoustic impulse acts on the system E_s generator–E_s load in the presence of this ambient field, and the ambient field adds just to the additionally generated electric field in the E_s load, then the drift velocity could exceed the sound velocity and the generation of the FB instability becomes possible.

References

Alimov, O. A., M. B. Gokhberg, E. V. Liperovskaya, I. L. Gufeld, V. A. Liperovsky, and L. N. Rubzov, Anomalous characteristics of the mid-latitude *E*-layer before earthquakes, *Phys. Earth and Planet. Interior*, **57**, 76–81, 1989.

Andreeva, L. A., Yu. B. Burakov, L. A. Katasev, G. P. Comrakov, U. P. Nesterov, D. B. Uvarov, V. G. Khryulin, and Yu. R. Chasovitin, Rocket investigation of the ionosphere at midlatitudes, *Space Res.*, **11**, 1043–1050, 1971.

Blanc, E., Observations in the upper atmosphere of infrasonic waves from natural or artificial sources: A summary, *Ann. Geophysicae*, **3**, 673–688, 1985.

Fatkullin, M. N., T. I. Zelenova, V. K. Kozlov, A. L. Legen'ka, and T. N. Soboleva, *Empirical models of the mid-latitude ionosphere*, Nauka, Moscow, 1981.

Gershman, B. N., Ju. A. Ignat'ev, and G. Ch. Kamenetzkaya, *Formation Mechanism of the Ionospheric Sporadic E_s-Layer at Different Altitudes*, Nauka, Moscow, 1976.

Haldoupis, C., A review on radio studies of auroral *E*-region ionospheric irregularities, *Ann. Geophysicae*, **7**, 239–258, 1989.

Haldoupis, C., and K. Schlegel, A 50-MHz radio Doppler experiment for midlatitude *E*-region coherent backscatter studies: System description and first results, *Radio Sci.*, **28**, 959–978, 1993.

Jacobson, A. R., and P. A. Bernhardt, Electrostatic effects in the coupling of upper atmospheric waves to ionospheric plasma, *J. Geophys. Res.*, **90**, 6533–6541, 1985.

Liperovskaya, E. V., O. A. Pochotelov, M. A. Oleynik, O. A. Alimov, S. S. Pavlova, and M. Khakimova, Some effects in the sporadic ionospheric *E*-layer before an earthquake, *Izv. RAN Fiz. Zemli*, **11**, 86–88, 1994.

Liperovsky, V. A., O. A. Pochotelov, and S. L. Shalimov, *Ionospheric Precursors of Earthquakes*, Nauka, Moscow 1992.

Liperovsky, V. A., C. V. Meister, Influence of collisional heating on the current generation in moving midlatitude sporadic *E*-layers, *Adv. Space Res.*, **18**, 93–97, 1995.

Manson, A. H., C. E. Meek, R. A. Vincent, R. L. Craig, A. Philips, G. J. Fraser, M. J. Smith, J. L. Fellous, M. Massebeuf, E. L. Fleuning, and S. Chandra, Comparison between Reference Atmosphere winds and radar winds from selected locations, *Adv. Space Res.*, **10**, 233–243, 1990.

Najita, K., P. F. Weaver, and P. C. Yuen, A tsunami warning system using an ionospheric technique, *IEEE Proc.*, **62**, 563–567, 1974.

Pocock, E., 144-MHz sporadic *E*, *QST*, 37–41, 1994.

Rowe, Jr. J.F., A statistical summary of Arecibo nighttime *E*-region observations, *J. Geophys. Res.*, **78**, 6811–6817, 1973.

Schlegel, K., A possible effect of magnetospheric convection on ionospheric conductivities, *Ann. Geophysicae*, **2**, 207–210, 1984.

Schlegel, K., and C. Haldoupis, Observation of the modified two-stream plasma instability in the mid-latitude E-region iono-sphere, *J. Geophys. Res.,* **99**, 6219–6226, 1994.

Sprenger, K., Diurnal and seasonal variations of occurence of sporadic *E*-layers over central Europe, *Gerlands Beitr. Geophys.*, **90**, 305–315, 1981.

Toroshelidze, T. I., and L. M. Fishkova, An analysis of the middle and upper atmosphere night airglow oscillations preceding earthquakes, *Dokl Acad Sci USSR*, **302**, 313–316, 1988.

Tshavdarov, S. S., Ju.K. Tshasovitin, S. P. Tshernysheva, and V. M. Sheftel, *Mid-Latitude Ionospheric Sporadic E-Layer*, Nauka, Moscow, 1975.

Tsunoda, R. T., S. Fukao, and M. Yamamoto, Modeling of quasi-periodic backscatter from E-region field-aligned irregularities in mid-latitude sporadic E, *Proc. COSPAR Coll. Low-Latitude Ionospheric Physics*, Taipei, Taiwan, 9.–12. Nov. 1993, pp. 183–194, 1993.

Tsunoda, R. T., S. Fukao, and M. Yamamoto, edited by Fu-Shong Kuo, Institute of Space Science, National Central University, Chung-Li, Taiwan.

Völk, H. J., and G. Haerendel, Striations in ionospheric ion clouds, *J. Geophys. Res.*, **76**, 4541–4559, 1971.

Walterscheid, D., A. Schubert, Nonlinear evolution of upward propagating gravity wave: overturning, convection, transience and turbulence, *J. Atmos. Sci.*, **47**, 101–125, 1988.

Whitehead, J. D., Recent work on mid-latitude and equatorial sporadic-E, *J. Atmos. Terr. Phys.*, **51**, 401–424, 1989.